



1

1 Using data and model to infer climate and environmental changes during the
2 Little Ice Age in tropical West Africa

3
4 Anne-Marie Lézine¹, Maé Catrain¹, Julián Villamayor^{1,2} and Myriam Khodri¹.

5
6 1. Laboratoire d'Océanographie et du Climat. Expérimentation et Approche numérique/IPSL.
7 Sorbonne Université-CNRS-IRD-MNHN. 4 Place Jussieu. 75005. Paris. France

8 2. Department of Atmospheric Chemistry and Climate, Institute of Physical Chemistry
9 Rocasolano, CSIC, Madrid, Spain.

10

11 **Abstract**

12 Here we present hydrological and vegetation paleo-data extracted from 28 sites in West Africa
13 from 5° S to 19° N and the past1000/PMIP4 IPSL-CM6A-LR climate model simulations covering
14 the 850-1850 CE period to document the environmental and climatic changes that occurred
15 during the Little Ice Age (LIA). The comparison between paleo-data and model simulations
16 shows a clear contrast between the area spanning the Sahel and the Savannah in the North,
17 characterized by widespread drought, and the equatorial sites in the South, where humid
18 conditions prevailed. Particular attention was paid to the Sahel, whose climatic evolution was
19 characterized by a progressive drying trend between 1250 and 1850CE. Three major features
20 are highlighted: (1) the detection of two early warning signals around 1170 and 1240CE
21 preceding the onset of the LIA drying trend; (2) an irreversible tipping point at 1800-
22 1850CE characterized by a dramatic rainfall drop and a widespread environmental
23 degradation in the Sahel; and (3) a succession of drying events punctuating the LIA, the major
24 of which was dated around 1600CE. The climatic long-term evolution of the Sahel is associated
25 with a gradual southward displacement of the Inter-Tropical Convergence Zone induced by
26 the radiative cooling impacts of major volcanic eruptions that have punctuated the last
27 millennium.

28

29 **1. Introduction**

30 Precipitation in tropical West Africa is closely related to the West African Monsoon (WAM)
31 system, created by the temperature land-sea contrast between the tropical Atlantic and the
32 west of the African continent (Nicholson, 2013). The WAM long-term variability during the
33 20th century has focused much attention due to the severe consequences in the Sahel semi-
34 arid region, which experienced a long period of drought in the 1970-80s (Folland et al. 1986;
35 Giannini et al. 2003). It is broadly accepted that these changes were mainly driven by the sea
36 surface temperature (SST) variability (Folland et al. 1986; Mohino et al. 2011; Rodríguez-
37 Fonseca et al. 2015), amplified by land surface processes (Giannini et al. 2003; Kucharski et al.
38 2013). However, only a few works document the WAM variability prior to the 20th century
39 (Nicholson et al. 2012; Gallego et al. 2015; Villamayor et al. 2018) due to the little information
40 covering the 19th century and beyond. The paleo-archives are rare, often incomplete, and
41 suffer from often poorly constrained chronologies. Moreover, these archives are rarely direct
42 records of climate parameters, but indirect ones, namely historical, biological, or
43 sedimentological. They integrate not only changes in environmental parameters but also the
44 vital effect of species, the vulnerability or the resilience of ecosystems and the cultural
45 adaptations of populations. Here we use pollen and other environmental proxies as well as

¹ Corresponding author : anne-marie.lezine@locean.ipsl.fr



46 historical chronicles to document the last millennium with a special focus on the period from
47 1250 to 1850 CE including the transition between the Medieval Climate Anomaly (MCA; 950-
48 1250CE) and the Little Ice Age (LIA; 1450-1850CE) periods characterised by global
49 temperatures respectively above and below average (Nash et al. 2016; Villamayor et al. sub.).
50 The aim of this review is not to record the climate variability at interannual scale but to discuss
51 the timing, distribution and magnitude of the major secular environmental changes which
52 punctuated the LIA in northern tropical Africa with a focus on the regional biomes and
53 hydrological systems responses times to rainfall anomalies.

54 2. Material and method

55 2.1 Paleo-data

56

57 This paper uses compilations of paleo-records from different sources with the highest
58 available resolution (Table 1; Fig. 1). These data have the advantage of providing continuous
59 records over the last millennium, but their temporal resolution is generally mostly
60 (multi)decadal to centennial : pollen data are used for vegetation reconstructions (Elenga
61 1992 ; Reynaud-Farrera et al. 1996; Ballouche 1998; Vincens et al. 1998; Salzmann et al. 2005;
62 Ngomanda et al. 2007; Waller et al. 2007; Brncic et al. 2009; 2017; Lézine et al. 2011; 2013;
63 2019; Lebamba et al. 2016; Tovar et al. 2019; Fofana et al. 2020; Catrain 2021), and
64 micropaleontological, sedimentological and geochemical data to capture hydrological and
65 climatic changes (Bertaux et al. 1998 ; Holmes et al. 1999 ; Street-Perrott et al. 2000 ; Schefuss
66 et al. 2005 ; Wang et al., 2008 ; Shanahan et al. 2009 ; Mulitza et al. 2010 ; Nguetsop et al.
67 2010 ; 2011 ; 2013 ; Carré et al. 2019 ; Lézine et al. 2019 ; Fofana et al. 2020 ; Catrain 2021).
68 Compilations of historical chronicles (Nicholson 1978; 1980; 2013; Nicholson et al. 2012;
69 Coquery-Vidrovitch 1997; Maley and Vernet 2013) and instrumental records (Gallego et al.
70 2015) have also been examined, although the first are based on records of extreme events
71 only (droughts, floods) and the second are limited in their temporal coverage. All these data
72 are also scattered in a few limited areas of the Sahel (Senegal, Southern Mauritania, Niger
73 River inner loop, Lake Chad basin) with possible redundancies.

74 The resulting data set is highly heterogeneous. Therefore, the data have been homogenized
75 as follows: (1) only records covering the interval between 900 CE and present day with at least
76 a 100-year temporal resolution have been taken into account, (2) in order to evaluate the
77 relative amplitude of the environmental/climate change, we build a 6-point scale ranging from
78 0, corresponding to the most degraded environment (e.g., drying of lakes, salinization of
79 water, increase of dust transport, degradation/opening of the vegetation cover) or the driest
80 climate, up to 6, which refers to the less degraded environment (e.g., high lake level, fresh
81 water, dense vegetation cover) or the wettest climate.

82

Site name	proxy	latitude	longitude	reference	Sector/vegetation zones
Lake Yoa	Pollen/sediment	19.057621	20.500690	Lézine et al. 2011	Sahara (Desert)
GeoB9501	Dust fraction	16.83333	-16.73333	Mulitza et al. 2010	Sahel
St Louis	Pollen/Diatom	16.03508	-16.48382	Fofana et al. 2020	Sahel (grasslands and wooded grasslands)



3

Mboro-Baobab	Pollen/Diatom	15.149132	-16.909275	Lézine et al. 2019	Sahel (grasslands and wooded grasslands)
Oursi	Pollen	14.65283	-0.486	Ballouche 1998	Sahel (grasslands and wooded grasslands)
Diron Boumak	Geochemistry	13.835809	-16.498372	Carré et al, 2019	Sahel/Savannah boundary
Lake Jikaryia	Sediment/Mineral-magnetic	13.3136667	11.077	Waller et al. 2007; Wang et al. 2008	Sahel (grasslands and wooded grasslands)
Lake Bal	Ostracods/Chemistry	13.304	10.943	Holmes et al. 1999	Sahel (grasslands and wooded grasslands)
Lake Kajemaru m	Dust fraction/Geochemistry	13.303	11.024	Street-Perrott et al. 2000	Sahel (grasslands and wooded grasslands)
Lake Chad	Historical	13.053472	14.463469	Maley and Vernet 2013	Sahel (grasslands and wooded grasslands)
Lake Mbalang	Pollen/Diatoms	7.316	13.733	Vincens et al. 2000; Nguetsop et al. 2011	Savannah
Lake Tizong	Pollen/Diatoms	7.25	13.583	Nguetsop et al. 2013; Lebamba et al. 2016	Savannah
Lake Sélé	Pollen	7.15	2.433	Salzmann et al. 2005	Savannah
Lake Bosumtwi	Geochemistry	6.5	-1.416	Shanahan et al. 2009	Central Africa (lowlands) (Equatorial forests)
Mbi	Pollen	6.089273	10.348549	Lézine et al., in press	Central Africa (highlands) (Afromontane forests)
Lake Bambili	Pollen/ Geochemistry	5.936	10.242	Lézine et al. 2013	Central Africa (highlands) (Afromontane forests)
Lake Petpenoun	Pollen	5.64147	10.64531	Catrain 2021	Savannah

3



4

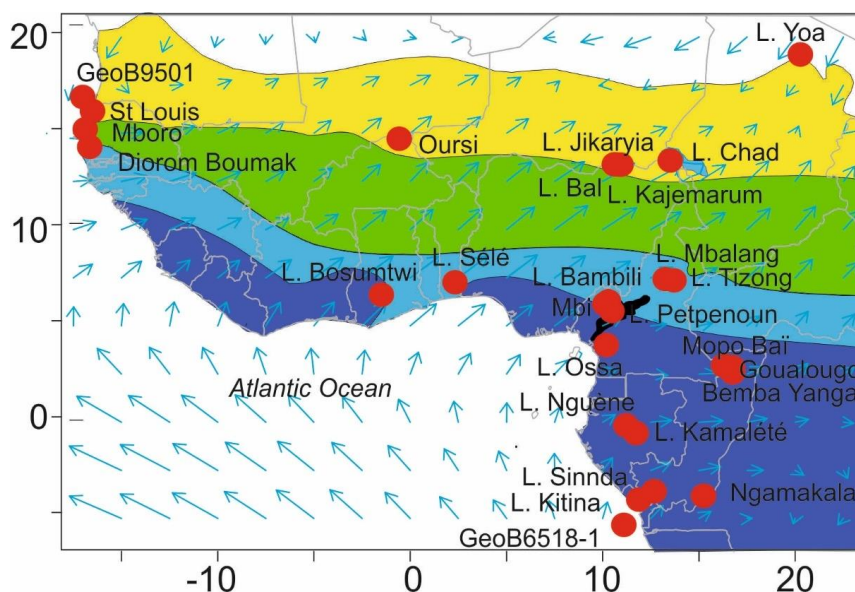
Lake Ossa	Pollen/Diatoms	3.800	10.75	Reynaud Farrera et al. 1996; Nguetsop et al. 2010	Central Africa (lowlands) (Equatorial forests)
Mopo Bai	Pollen/Geochemistry	2.240	16.261388	Brncic et al. 2009	Central Africa (lowlands) (Equatorial forests)
Bemba Yanga	Pollen	2.18726	16.52513	Tovar et al. 2019	Central Africa (lowlands) (Equatorial forests)
Goualougo	Pollen	2.0875	16.54722	Brncic et al. 2017	Central Africa (lowlands) (Equatorial forests)
Lake Nguène	Pollen	-0.2	10.466	Ngomanda et al. 2007	Central Africa (lowlands) (Equatorial forests)
Lake Kamalété	Pollen	-0.7166	11.7666	Ngomanda et al. 2007	Central Africa (lowlands) (Equatorial forests)
Lake Sinnda	Pollen/Sediment	-3.836111	12.8	Bertaux et al. 1996 ; Vincens et al. 1998	Central Africa (lowlands) (Equatorial forests)
Ngamakala	Pollen	-4.075	15.38333	Elenga 1992	Central Africa (lowlands) (Equatorial forests)
Lake Kitina	Pollen/Sediment	-4.27	12	Bertaux et al. 1996 ; Elenga et al. 1996	Central Africa (lowlands) (Equatorial forests)
GeoB6518-1	Alkenone / Geochemistry	-5.588333	11.221667	Schefuss et al. 2005	Central Africa

83
 84 Table 1: Geographical positions, type and references of paleo-records used in this study (see
 85 Fig. 1).
 86

4



5



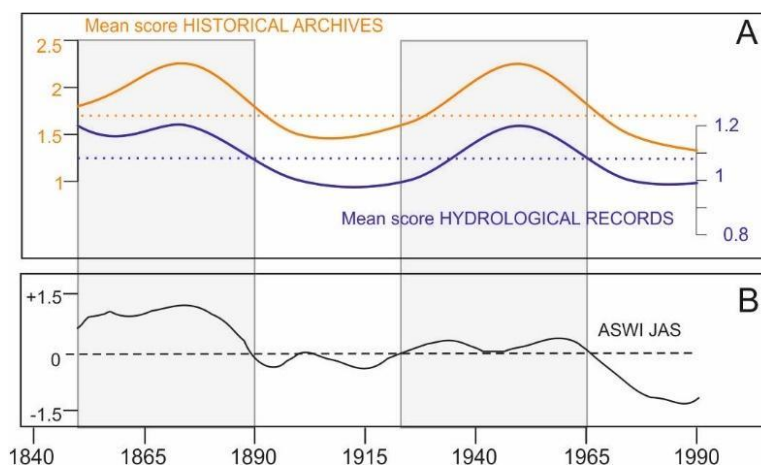
87
88 **Figure 1:** Map showing the location of paleorecords available in tropical West Africa
89 documenting the last millennium (Table 1). Blue arrows indicate the strength and direction of
90 the main 925 hPa monsoonal winds during boreal summer, i.e., the WAM rainy season (NCEP-
91 DOE AMIP-II Reanalysis (Kanamitsu et al., 2002)). In color, vegetation units from White (1983):
92 dark blue: Guineo-Congolian rainforest; light blue: Sudano-Guinean woodland and wooded
93 grassland (here referred to as Savannah (vegetation) zone); green: Sudanian woodland and
94 wooded grassland ; yellow: Sahelian grassland and wooded grassland. black: Afromontane
95 forest.

96
97 In order to verify whether the methodology employed is realistic and provides reliable
98 indications of environmental change for the period prior to the instrumental records, scores
99 of the WAM rainy season (July to September) multidecadal hydrological changes from natural
100 archives and historical data (Table 1) in the Sahel are compared to the African Southwesterly
101 Index (ASWI) developed by Gallego et al. (2015) over 1840-1990 CE. The ASWI was validated
102 against instrumental observations as a good measure of WAM intensity during the rainy
103 season over the instrumental period (Gallego et al. 2015). Positive values of the ASWI indicate
104 periods when the monsoon is well established over the Sahel, and thus define periods of heavy
105 rainfall in the region, which is consistent with observational data (Descroix et al., 2015). Figure
106 2 shows that our historical records give a magnitude of dry and wet anomalies that reflects
107 the sensitivity of populations to periods of drought or flooding. Our assessment of hydrological
108 conditions based on natural archives reflects historical records variations but with a somewhat
109 weaker magnitude. This is probably due to the much lower temporal resolution of the
110 available data (25-50 yrs on average). It is also worth noting that the lake data corresponds
111 to a precipitation/evaporation balance and not the precipitation amounts at a given site.
112 Nevertheless, the curves are remarkably similar and point to wet periods centred ca 1875 and
113 1950 CE.
114

5



6



115
116

117 **Figure 2:** Observed and reconstructed rainfall anomalies over the Sahel during the 1840-1990
118 CE period. (A) the mean scores from historical (yellow curve) and natural archives (blue curve)
119 for the Sahel (Nicholson, 1978; 1980; Nicholson et al. 2012; 2013; Coquery-Vidrovitch, 1997;
120 Holmes et al., 1999; Street-Perrott et al. 2000; Waller et al. 2007; Wang et al. 2008; Mulitza et
121 al. 2010; Maley and Vernet, 2013; Lézine et al. 2019). The dotted yellow and blue lines
122 correspond respectively to the historical and paleohydrological archives mean scores during
123 the period 1850-1990CE. They allow identifying anomalously wet and dry periods. (B) The
124 African Southwesterly Index (ASWI) developed by Gallego et al. (2015) as a measure of rainfall
125 anomalies in Sahel during the WAM rainy season (July to September).

126

127

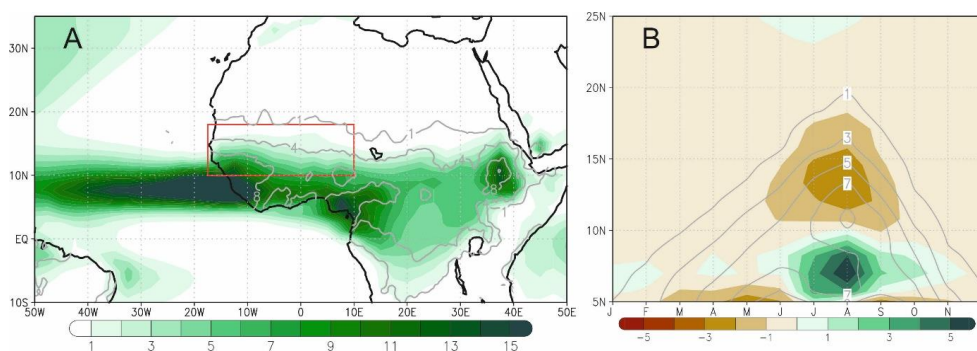
2.2 Model experiments

128 In this study we compare reconstructed environmental changes in Western Africa to those
129 simulated in the past1000 model experiment covering the 850-1850 CE climate performed as
130 part of 4th phase of the Paleoclimate Modelling Intercomparison Project (PMIP4; Jungclaus et
131 al. 2017; Kageyama et al. 2017) by the IPSL-CM6A-LR model version developed for the Coupled
132 Model Intercomparison Project phase 6 (CMIP6) at Institut Pierre-Simon Laplace (Boucher et
133 al. 2020; Lurton et al. 2020). The IPSL-CM6A-LR model couples the atmospheric component
134 LMDZ (Hourdin et al. 2020) to the land surface model ORCHIDEE (d'Orgeval et al., 2008) and
135 to the ocean model NEMO, which includes other models to represent sea-ice interactions
136 (Rousset et al., 2015) and biogeochemistry processes (Aumont et al. 2015). The atmospheric
137 and land-surface grid have a resolution of 2.5° in longitude and 1.3° in latitude with 79 vertical
138 layers. The oceanic component has 75 vertical levels with a mean spatial horizontal resolution
139 of about 1° and a refinement of 1/3° near the equator. This model reproduces fairly well the
140 ENSO seasonality despite the sea surface temperature anomalies extending too westward in
141 the central Pacific during El Niño events. The spatial pattern of the AMV teleconnection in the
142 Pacific is consistent with observations but the tropical Atlantic variability is relatively weaker.
143 Unlike most current state-of-the-art CMIP6 models, the IPSL-CM6A-LR model simulates a
144 predominant secular variability in the Atlantic with AMV peaks separated by about 200 years
145 (Boucher et al., 2020).

146 The past1000 IPSL-CM6A-LR model experiment is designed to simulate the climate response
147 to natural forcings recommended by PMIP4 (Jungclaus et al. 2017) and covering the pre-



148 industrial millennium (850-1849CE), namely the time varying astronomical parameters, the
149 trace gases (Meinshausen et al. 2017; Matthes et al. 2017), the eVolv2k volcanic forcing
150 (Toohey and Sigl 2017), the SATIRE-M 14C solar activity with an adaptation of the spectral
151 irradiance to the CMIP6 *historical* forcing and the land use forcing (Lawrence et al. 2016).
152 Three past1000 IPSL-CM6A-LR model simulations have been performed and branched off from
153 various initial conditions in a 600 years long spinup run with fixed external radiative forcing to
154 the year 850 CE. This spinup run, itself branched off from the IPSL-CM6A-LR pre-industrial
155 control (piControl) run with constant external radiative forcing, has been performed to avoid
156 any spurious drift in the past 1000 experiments that could be related to the adjustment of the
157 slow components of the climate system (such as the ocean), to the different radiative balance
158 at the beginning of the last millennium as compared to the pre-industrial levels.
159
160



161
162

163 **Figure 3:** Climatological bias of simulated monthly precipitation. A) JAS mean averaged across
164 (colors) the 2000 year piControl run and (contours) the 1891-2019 period in GPCPv2020
165 observational database. B) (colors) Meridional seasonal cycle of the 10° W – 10° E mean model
166 bias (simulation minus observations) compared to (contours) the GPCPv2020 climatology. All
167 units are mm/day. Red box in (A) indicates the Sahel region (17.5°W-10°E; 10°-18°N).

168

169 The IPSL-CM6A-LR model reproduces the observed climatological distribution of maximum
170 rainfall across West Africa during the WAM rainy season (Fig. 3A). The timing of the simulated
171 WAM seasonal cycle is also in good agreement with observations, with a well-defined onset
172 of the rainy season in July and then a demise after September (Fig. 3B). However, the
173 northward shift of maximum rainfall over the Sahel (north of 10°N) during the rainy season is
174 slightly underestimated by the model, resulting in a climatological rain belt over West Africa
175 that is slightly more constrained to tropical regions compared to observations and dryer Sahel
176 on average. However, the well-characterized WAM seasonal timing suggests that there are no
177 remarkable biases affecting the simulated precipitation variability.

178

179 Then, to characterize the simulated Sahel rainfall variability over the past millennium and
180 contrast to the reconstructed environmental series, an index is performed using the past1000
181 ensemble-mean precipitation anomalies (relative to the piControl average) from July to
182 September (JAS), area-weighted and averaged across the Sahel region (red box in Fig. 3A). In
183 order to highlight the variability at decadal to longer time scales, the index is low-pass filtered
184 using a 10-year moving mean. In turn, the ensemble-mean anomalies help highlight the
185 changes in precipitation induced by external forcing, common across the different



186 realizations, against internal variability. Therefore, the ensemble-mean past1000 index of
187 Sahel precipitation represents the variability at decadal to longer time scales modulated by
188 internal processes and external natural forcings, such as the radiative forcing induced by large
189 volcanic eruptions.

190

191 3. Results

192 3.1 The hydrological records

193

194 The hydrological records provide a contrasting picture from one region to another: the Sahel,
195 the Sudano-Guinean Savannah zone and the tropical forests. They also reveal some local
196 exceptions. As already noted (e.g., Vincens et al. 1999), the local hydrogeological context may
197 strongly affect the individual response of lakes and wetlands to rainfall variations and partly
198 explains this apparent heterogeneity.

199 The main characteristics of the hydrological evolution in the Sahel, in the Savannah zone and
200 in low and high altitude equatorial forests can be summarized as follows (Fig. 4):

201 • Data from the central and western Sahel (Fig. 4A) point to a relatively dry period at the
202 end of the first millennium (900CE) at Bal, Kajemarum and in the Senegal River
203 watershed (GeoB9501). A wet period followed, already present at Mboro near the
204 littoral, which lasted up to 1350CE. Except at Kajemarum and Jikarya, where
205 hydrological conditions remained relatively stable, a gradual trend toward increased
206 aridity is recorded in two steps dated ca. 1625CE and 1800CE, respectively. Then,
207 during the last two centuries, only minor fluctuations occurred in a general context of
208 widespread aridity.

209 In the lake Chad area, Maley and Vernet (2013) depict a rather different and complex
210 history probably due to the variety of the archives they used (both historical and
211 natural) and also to the complexity of the hydrology of this immense water body
212 (Pham-Duc et al. 2020) fed by underground waters and by rivers of distant
213 geographical origin. The authors identify two major periods of flooding in the lake
214 Chad area: from the onset of the millennium to ca. 1200CE, then between 1600 and
215 1700CE, with a series of dry periods in between then from 1700CE onwards.

216 • Only three sites document the hydrological evolution of the Savannah zone south of
217 the Sahel (Fig. 4C). These sites are located in the centre of the savannah zone (White
218 1985): two crater lakes on the Adamawa plateaus (Mbalang and Tizong) and the other
219 at the mouth of the tributary of Lake Petpenoun in the Grassfields region of Cameroon.
220 The Adamawa lakes do not show any significant hydrological changes throughout the
221 last millennium. In contrast Petpenoun records a clear evolution towards aridity which
222 started ca. 1425CE and culminated ca. 1650CE up to the present day.

223 • Diorom Boumak (Fig. 4B) is situated at the southern boundary of the Sahel, in the
224 littoral mangrove of the Saloum estuary. In contrast to the other sites from the Sahel
225 and savannah zone this site records a remarkable wet period between 1500CE and
226 1800CE. As elsewhere however, aridification started ca. 1800CE.

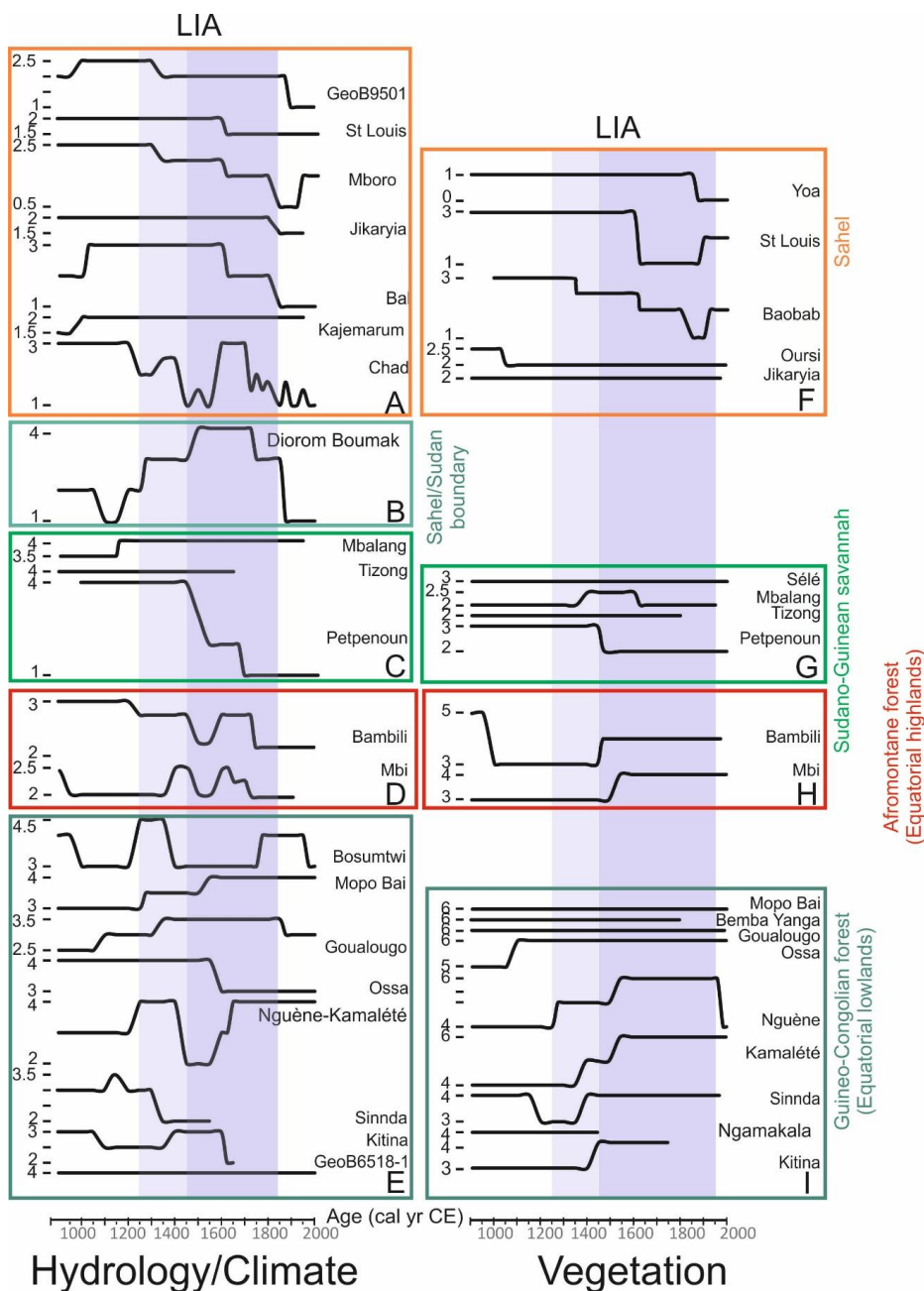
227 • The equatorial region is characterized by contrasting hydrological situations (Fig. 4E).
228 Low lake levels are recorded at Bosumtwi, Mopo Bai, Goualougo, Nguène-Kamalété
229 during a period centred around 1100CE in contrast to Sinnda and Kitina where moist
230 conditions occurred. Moisture increased as soon as 1350CE at Goualougo and
231 continued up to 1400CE at Mopo Bai and Kitina. Then, there is a clear opposition
232 between Sinnda, Nguène-Kamalété, Bosumtwi and Ossa where low lake levels



233 occurred during a dry phase between ca 1350 and 1700CE and Mopo Bai, Goulougo
234 and Kitina which are characterized by wetter conditions. In any case, the marine record
235 at the mouth of the Congo River (GeoB6518-1) suggests that all these hydrological
236 variations in the equatorial lowlands remained of relatively low amplitude.
237 In the Cameroon highlands (Fig. 4D), hydrological conditions steadily declined as
238 shown at lake Bambili, starting from ca. 1250 and culminating ca. 1675CE. This gradual
239 trend is interrupted ca. 1500CE by a more pronounced phase of lake level lowering.
240 The Mbi swamp displays a rather different pattern: here, the water level was relatively
241 low throughout the whole last millennium except to two discrete wetter phases ca.
242 1450 and 1650CE.
243



10



244
 245
 246
 247
 248
 249
 250
 251

Figure 4: Mean scores of hydrological and vegetation changes along a North-South transect from the northern limit of the Sahel (Yoa) to the Congo basin (GeoB6518-1). Data are grouped within the phytogeographical entities defined by White (1983) in tropical Africa : Sahelian grassland and wooded grassland, Sudano-Guinean savannah, highland Afromontane forest, lowland Guineo-Congolian forest.



252 **3.2 Pollen data**

- 253 • In the open landscapes of the Sahara, Sahel and Savannah zones, vegetation changes
254 were of minor amplitude except at sites where gallery forests were previously well
255 developed. It is in the westernmost part of the Sahel that the most profound changes
256 in vegetation cover are recorded : In the Niaye area (Mboro) and in the Senegal river
257 delta (St Louis), the degradation of the landscape originated ca. 1300CE and
258 accelerated ca. 1600CE to a maximum reached ca. 1850CE (Fig. 4F). A discrete
259 vegetation recovery is then recorded in the 19th century. In contrast, sites from the
260 central Sahel (Oursi and Jikaryia) remained relatively stable throughout the last
261 millennium in spite of a slight degradation recorded at Oursi ca. 1050CE. North of the
262 Sahel (Yoa), the aridification of the desert landscape accelerated from the 19th century
263 onward. South of the Sahel, in the Savannah zone, lakes Tizong and Sélé do not record
264 any marked environmental change contrary to Petpenoun where a slight degradation
265 is recorded ca. 1425CE (Fig. 4G). At Mbalang, a discrete phase of vegetation recovery
266 occurred between ca 1400-1600CE.
- 267 • The forest cover remained roughly unchanged in the central forest massif (Mopo Baï,
268 Bamba Yanga. Goulalougo, Fig. 4I). In the western regions however, (Ngamakala,
269 Kitina, Lake Ossa, Nguène and Kamalété) a trend toward forest development started
270 ca. 1250-1350CE. In the Cameroon highlands (Fig. 4H), the forest development
271 occurred later, ca 1550-1500CE, after a phase of forest clearance from 1000 to
272 1450CE.

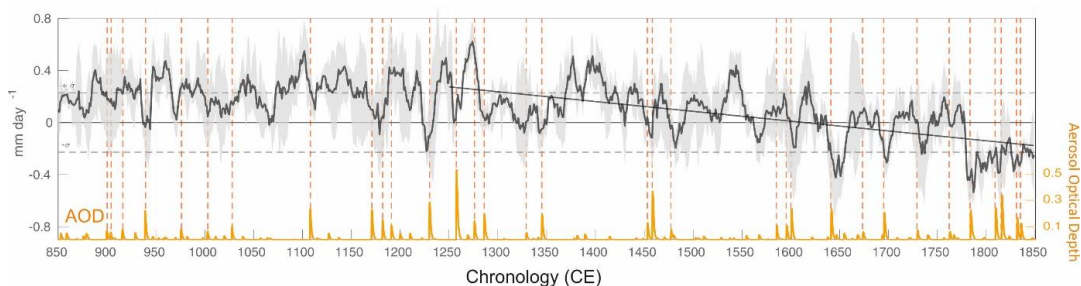
273 **3.3 Model results**

274

275 The index of the ensemble-mean Sahel JAS precipitation simulated over the past millennium
276 reveals a change from a relatively wet mean state in the MCA (950-1249 CE) to a drier one in
277 the LIA (1450-1849) (Fig. 5), suggesting a shift of the average WAM rainfall regime. Such
278 continuous decline presents a linear rate of the seasonal Sahel rainfall of -0.7 mm per decade
279 over 1250-1849CE, resulting in a 7% loss of the mean precipitation in the LIA relative to MCA
280 (Fig. 5). Regarding decadal variations, the ensemble-mean index of past1000 Sahel
281 precipitation almost doubles its variability in the LIA with respect to the MCA (the variance in
282 859-1249CE is 51% higher than in 1450-1849CE), which suggests a more unstable rainfall
283 regime, apart from drier on average, by the late past millennium in response to natural
284 external forcings. As shown by Villamayor et al. (2022), such a simulated long term drying
285 trend and increased LIA Sahel precipitation decadal variability is related to the volcanic forcing
286 influence on SSTs, which integrates the induced radiative cooling (Fang et al. 2021). The more
287 frequent large volcanic eruptions during the LIA, as compared to the MCA, is integrated by the
288 ocean long memory, leading to a gradual SST decrease that is more pronounced in the
289 Northern Hemisphere than the Southern Hemisphere. The relative North Atlantic SST cooling
290 trend along 850-1849CE, gradually promotes a southward shift of the Inter-Tropical
291 Convergence Zone (ITCZ) and a weakening of monsoon moisture inflow to Western Africa. The
292 long term WAM weakening is further amplified in the few years following any new large
293 volcanic event, which occurrences are indicated by the vertical dotted lines on Figure 5A. As a
294 consequence, more frequent negative rainfall anomalies lasting at least 5 consecutive years
295 are also evident during the LIA as compared to the MCA, with significant drying that can persist
296 up to 60 years around clusters of eruptions such as those of the 19th century.



297
298



299
300

301 **Figure 5:** Multidecadal Sahel rainfall variability in IPSL-CM6A-LR past1000 simulations. Black
302 line: 10-years low pass filtered index of anomalous JAS Sahel precipitation anomalies averaged
303 in boxed area in Figure 3 (i.e., 10°-18°N and 17.5°W-10°E). The black line corresponds to the
304 ensemble mean, the grey shading to the ensemble spread and diagonal line to the 1250-1849
305 CE linear fit. Dashed horizontal lines show the +/-standard deviation of the equivalent
306 piControl index. The volcanic forcing used in the IPSL-CM6A-LR model experiments is shown
307 by the orange curve as the globally averaged Aerosol Optical Depth (AOD). Red vertical dotted
308 lines indicate the occurrence of strong volcanic eruptions about the size or larger that the
309 Pinatubo eruption (June 1991) defined when the tropical (20°S-20°N) or northern extratropical
310 (50°N-90°N) mean AOD is larger than 0.1.

311

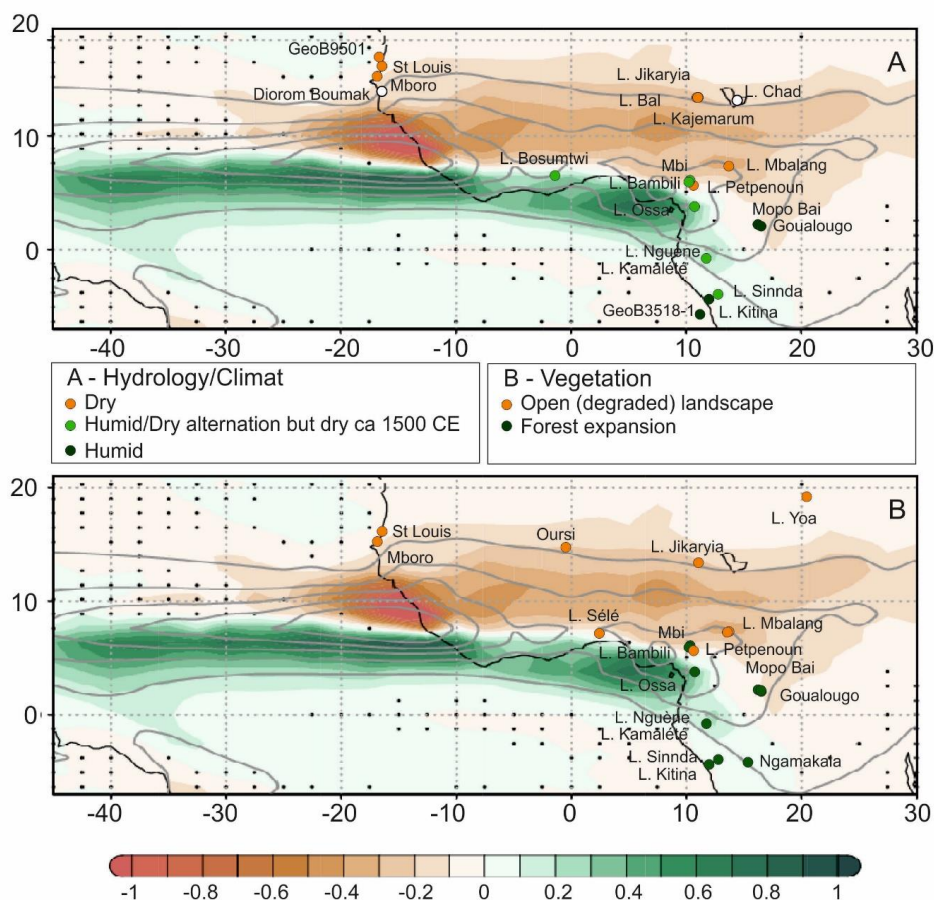
312 4. Discussion

313

314 4.1 Hydrology and Climate changes at secular timescale

315

316 Data and past1000 model simulations show a strong North-South contrast between the Sahel
317 and Savannah zones, both subjected to severe drying during the LIA, and the equatorial areas,
318 spanning the Gulf of Guinea coast, suggesting an overall change of the WAM.



319
 320

Figure 6: Distribution of JAS rainfall anomalies between the LIA (1450-1849 CE) and the MCA (950-1249 CE) as simulated by the IPSL-CM6A-LR model (shading, mm day⁻¹) compared to hydrological/dust (A) and vegetation (B) paleorecords during the LIA shown as dots following the same color scale as simulated anomalies. Grey contours indicate the piControl climatology from 2 mm day⁻¹ in intervals of 4 mm day⁻¹. Stippling indicates areas where the anomalies do not significantly emerge from the internal noise with 95% confidence level.

327

The difference between the simulated past1000 JAS precipitation during the LIA and the MCA shows a characteristic distribution of a weakened WAM associated with a southward shift of the ITCZ, with less rainfall across the Sahel and more in the Gulf of Guinea coast (Fig. 6). These simulated anomalies are consistent with the overall distribution of hydrological and vegetation proxy reconstructions.

333

4.1.1 Hydrology

334

Three major regions can be recognized from the paleohydrological records: The Sahel and Savannah zones, with drying trend; the center of the Congo Basin, which exhibit an opposite trend of increasing humidity; and the boundary between the dry and humid domains defined

335
 336
 337



338 by the equatorial sectors closest to the coast or in mountain, where an alternation of wet and
339 dry phases is recorded. Two paleo-records differ from this general picture: that of Lake Chad,
340 where a period of flooding is recorded ca 1600CE, and that of the Diorom Boumak, where the
341 LIA is entirely characterized by a wet period (Fig. 4). As evoked above, the multiple origins of
342 the data and the complex hydrological system of Lake Chad may have introduced a bias into
343 the hydrological record and may explain (at least partly) the difference with the other Sahelian
344 archives. It is also likely that the rivers that feed the lake, which originate from southern
345 regions (the Chari and Logone rivers and their tributaries), may have caused an influx of water
346 during the short humid phase recorded on the Cameroon highlands (Bambili and Mbi) ca
347 1600CE. The case of the Diorom Boumak site is more complex: the historical records
348 mentioned by Maley and Vernet (2013) or Carré et al. (2019), among others, indicate that the
349 Saloum sector was wetter than the rest of the Sahel during part of the 16th century, allowing
350 for the establishment of two harvests per year. This may have been due, according to Maley
351 and Vernet (2013), to the occurrence of two rainy seasons, one in summer linked to the WAM
352 and the other in winter due to intense « Heug » rains linked to northern depressions. Carré et
353 al. (2019) however do not consider any other cause than the intensification of the
354 WAM. Although the origin of this humid LIA in the Saloum still remains unexplained, the date
355 of its end, ca. 1800 CE, is consistent with all the other paleohydrological records from the
356 Sahel.

357

358 **4.1.2 Vegetation**

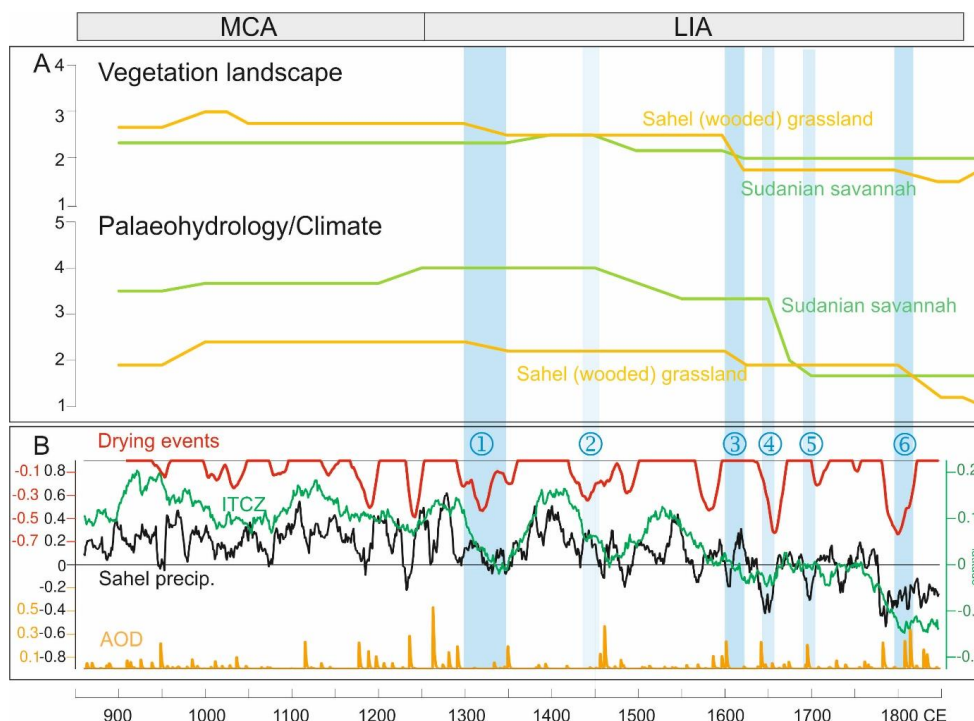
359 In the central Sahel, already degraded prior to the LIA (Lézine 2021), such as at Oursi, no
360 significant change occurred in the vegetation landscape which remained open throughout the
361 last millennium (Fig. 4B). The same pattern is observed in the wettest areas of the Congo Basin,
362 where the forests remained unchanged in composition and physiognomy (Tovar et al. 2019).
363 Elsewhere in the forest galleries of the Sahel and the Savannah zone (Mboro, St. Louis,
364 Petpenoun) the evolution of vegetation mirrored that of hydrological conditions while
365 recording a gradual degradation that culminated around 1800-1850 CE. In the westernmost
366 sector of the Sahel (Mboro, St Louis), the data suggest however a slight recovery of the
367 vegetation cover during the last few decades.

368 In contrast, both high and low elevation sites from the equatorial forest regions show an
369 opposite trend with marked forest recovery that began in the early years of the LIA and
370 accelerated around 1450CE. The forest expanded in the Equatorial lowlands despite increased
371 human presence has already been noted by Vincens et al. (1999). That means that the local
372 hydrological variations, and particularly the 1500 CE dry event, were of too small an amplitude
373 to impact forest dynamics. At most, a plateau in forest recovery is observed at that time
374 (Nguène, Kamalété). While the forest recovery was gradual at low altitudes, it seems to have
375 occurred more abruptly in the highlands.

376

377 **4.2 The chronology of events at multidecadal timescale: focus on the Sahel and Savannah** 378 **zone**

379



380
 381 **Figure 7:** Multiproxy records of hydrology and vegetation during the last millennium in the
 382 driest biomes (Sahel and Savannah zone) in western Africa (A) and long-term evolution of
 383 rainfall over the Sahel as simulated by the IPSL-CM6A-LR past1000 model (B). Panel B: (Black
 384 line) 10-year filtered ensemble-mean Sahel precipitation index (mm day^{-1}). (Green line) 50-
 385 year filtered anomalous latitudinal position of the JAS ITCZ (defined as the latitudinal
 386 maximum zonal-mean rainfall in $40^{\circ}\text{W}-10^{\circ}\text{E}$) in the past1000 simulations respectively to the
 387 piControl JAS mean position (in degrees of latitude). (Orange line) Global-mean AOD (volcanic
 388 forcing). (Red line) Sahel Drying Persistence Index defined as the 50-year running negative
 389 trend values over the Sahel ensemble-mean JAS precipitation index (mm day^{-1} per 50 years).
 390 Blue bars and numbers highlight the main climate/environmental degradation thresholds
 391 identified in the paleo-records.

392
 393 Environmental changes in the Sahel and Savannah zones during the LIA occurred in the context
 394 of widespread environmental degradation that followed the severe environmental crisis at
 395 the end of the African Humid Period (AHP; deMenocal et al., 2000). Between 3300 and 2500
 396 cal yr BP (Lézine, 2021), the forests and woodlands, that widely expanded across the plains
 397 and mountains of West Africa, strongly declined. This is particularly striking along the Atlantic
 398 coast of Senegal, between 15° and 17° N where specific environmental conditions related to
 399 the proximity of the sea and the presence of a water table near the surface favored the
 400 development of exceptionally dense forest galleries of humid tropical affinity during the AHP
 401 (Lézine 1989). As a result of this major environmental crisis, the Sahel and Savannah zone took
 402 on its modern aspect of semi-desert grassland and wooded grassland. In this context,
 403 discernible environmental fluctuations, particularly in vegetation, are of limited magnitude,
 404 with the exception of sectors where forest galleries were widely established during the AHP.
 405



406 To discuss the chronology of events that punctuated the LIA, paleo-data were averaged in
407 each geographical area (Sahel, Savannah zone) in the two categories covered by our study :
408 hydrology/climate and vegetation (Fig. 7A). A Drying Persistence Index was constructed from
409 our model results in order to quantify the Sahel precipitation deficit over at least 50-year
410 periods (red curve in Fig. 7B). It is defined at each year as the negative linear trend of the Sahel
411 ensemble-mean JAS precipitation (black curve in Fig. 7B) across the 50 previous years. We use
412 50 years to be consistent with the multi-decadal to centennial temporal resolution of the
413 paleo-data.

414 The past1000 simulations represent several drying events of various amplitude and duration
415 during the MCA that do not correspond to any major change in the vegetation of the Sahel
416 and Savannah zone. Instead, the environment in these two areas appears to be characterized
417 by a relatively stable humid regime (Fig. 7A). This is coherent with the rainy mean state
418 represented by the past1000 simulations over the MCA, which is associated with an
419 anomalous northward ITCZ position (green curve in Fig. 7B) all over this period compared to
420 the LIA.

421 At the end of the MCA, two early warning signals (Lenton 2011) of Sahel drying events centred
422 at 1170 and 1240 CE are identified in our model experiments. The intensity and brevity of
423 these two events contrast with the minor dry phases identified prior to the LIA since the onset
424 of the last millennium. The Drying Persistence Index at these two events, which timing
425 coincides with the occurrence of large clusters of volcanic eruptions (orange curve Fig. 7B),
426 reaches over -0.3 mm day^{-1} across 50 years. Both events preceded the onset of the LIA gradual
427 drying trend starting at 1250CE. This drying trend was sustained by the southward migration
428 of the ITCZ which shifts south of the piControl mean position at 1600 CE. It is consistent with
429 the continuous degradation of hydrological and vegetation conditions since 1250 CE in the
430 Sahel and Savannah zone identified in our multi-proxy records.

431 Several abrupt drying events larger than those identified during the MCA punctuated the LIA,
432 some of which reaching over -0.5 mm day^{-1} across 50 years. Despite the difference in temporal
433 scale between the two approaches used here, there is a striking agreement between the major
434 simulated droughts and the environmental degradation steps in our paleorecords (blue bars
435 in Fig. 7). These degradation periods, in turn, span the largest eruptions from ca. 1250 to ca.
436 1850CE, which are associated with the multi-decadal variability of Sahel precipitation over the
437 past millennium in PMIP4 multi-model experiments (Villamayor et al. sub.).

438 **4.2.1 Steps in the degradation of the climate and the environment in the Sahel**

439 Three major steps are identified:

- 440 - The first dramatic environmental degradation occurred between 1290 and 1350 CE
441 (event 1), i.e., ca. 50 years after the first warning signal and lasted about 60 years. Dust
442 fluxes to the ocean, which had stabilized during the medieval warm period, increased
443 (Mulitza et al. 2010) whereas lake levels dropped in the interdunal depressions in the
444 western Sahel leading to the salinization of the waters (Lézine et al. 2019).
- 445 - The second stage in the degradation of environmental conditions occurred ca 1600CE
446 (event 3). The environmental degradation was common to the entire Sahel (Ba,



447 Mboro, St Louis) while corresponding to a major collapse of the forest galleries at
448 Mboro. Here also, a time lag of ca. 50 years can be observed between the onset of a
449 drought phase and the response of the vegetation.

450 - The ultimate environmental threshold is recorded ca 1800CE (event 6). It resulted in
451 the widespread lowering of lake levels, the massive contribution of dust to the ocean,
452 and the irreversible destruction of forest galleries in the western Sahel in response to
453 an abrupt drop in rainfall ca 1800CE, already observed by Carré et al. (2019) in the
454 Saloum river delta. By accounting for a catastrophic decrease in precipitation of -0.6
455 mm day⁻¹ over 50 years in our model experiments, this climatic tipping point related
456 to closely spaced large volcanic eruptions (starting with Laki eruption in 1783 CE
457 followed by the eruptions cluster over the 1809-1835 CE period including the 1815
458 Tambora event), at the origin of the modern environmental conditions in the Sahel,
459 was twice as large as the early warning signals identified at the end of the MCA.

460 Our data-model comparison suggests that there was a time lag of several decades
461 (typically 50 years) between the climate signal and the environmental response. If this
462 time lag is highly probable, its duration and origin require further investigation. It may
463 indeed result from the resilience of plants to climate change but we cannot exclude the
464 memory effect of aquifers already observed by Aguiar et al. (2010) that may induce a delay
465 between the climate signal and its effects on ecosystems. The uncertainty associated with
466 the ages, whether it comes from the data or from the modelling, can also play a role by
467 increasing or reducing this response time.

468

469 **4.2.2 The Savannah zone:**

470

471 As the ITCZ moved to more southerly latitudes, some of the drought events reconstructed in
472 the Sahel had a major impact in the Savannah zone. Here, data is particularly sparse and, as in
473 the Sahel, changes in vegetation are hardly distinguishable in these already highly degraded
474 environments, such as at Lake Sélé (Salzmann et al. 2005). It is at Lake Petpenoun (Catrain
475 2021) that the evidence is the clearest due to the presence of a gallery forest and pronounced
476 hydrological changes at the core site.

477 We find that the last step of degradation of the savannah vegetation occurred during event 3
478 also observed in the Sahel. Events 2 (1447-1493CE), 4 (1643-1657CE) and 5 (1691-1707CE)
479 correspond only to phases of hydrological degradation that are not reflected in the regional
480 vegetation. Data are still too rare to generalize this observation to the entire Savannah zone
481 and could only account for local conditions.

482

483 **5. Conclusion**

484

485 Despite the uncertainties associated with data scarcity and heterogeneity, our study shows a
486 remarkable agreement between the data and our past1000 model experiments for
487 reconstructing the climate and environmental changes in response to natural forcing that
488 characterized the LIA in western Africa. It highlights a North-South contrast between the
489 dryness of the Sahel and the humidity of the equatorial zone. Despite the major difficulty
490 related to the type of vegetation at play in the Sahel and the Savannah zone already degraded
491 since the end of the AHP, major steps in the degradation of the environment can be identified.
492 Our most remarkable results consists in (1) the identification of two early warning signals at



493 1170 and 1240CE, i.e. prior to the progressive LIA drying of the Sahel that lead to the climatic
494 tipping point at 1800-1850CE. This tipping point marks the setting of arid conditions (the driest
495 condition since 850CE) which still persist today; (2) the identification of abrupt drought events
496 which punctuated the LIA, the most important of them has impacted both the Sahel and the
497 Savannah zone ca. 1600CE. The consistency between proxy records and our model
498 experiments suggests a strong role of large volcanic eruptions in shaping Sahel environmental
499 changes over the pre-industrial millennium. Further work relying in large ensembles of climate
500 and vegetation models will help assess such hypothesis.

501

502 **Code availability**

503

504 The IPSL-CM6A-LR model code used in this work was frozen (version 6.1.0) and subsequently
505 altered only for correcting diagnostics or allowing further options and configurations. Versions
506 6.1.0 to 6.1.11 are therefore bit-reproducible for a given domain decomposition, compiling
507 options and supercomputer. LMDZ, XIOS, NEMO and ORCHIDEE are released under the terms
508 of the CeCILL licence. OASIS-MCT is released under the terms of the Lesser GNU General Public
509 License (LGPL). IPSL-CM6A-LR code (version 6.1.0) is publicly available through Apache
510 Subversion (svn) control system, with the following command lines under Linux: `svn co`
511 `http://forge.ipsl.jussieu.fr/igcmg/svn/modipsl/trunk modipsl; cd modipsl/util; ./model`
512 `IPSLCM6.1.11-LR` (IPSL-CM model development team, 2021). The `mod.def` file provides
513 information regarding the different revisions used, namely (1) NEMOGCM branch
514 `nemov36STABLE` revision 9455; (2) XIOS2 branches/`xios-2.5` revision 1873; (3) IOIPSL/src svn
515 tags/`v224`; (4) LMDZ6 branches/`IPSLCM6.0.15` rev 3643; (5) tags/`ORCHIDEE20/ORCHIDEE`
516 revision 6592; (6) OASIS3-MCT 2.0branch (rev 4775 IPSL server). The login and password
517 combination requested at first use to download the ORCHIDEE component is “anonymous”
518 and “anonymous”. We recommend referring to the project website,
519 <http://forge.ipsl.jussieu.fr/igcmg/doc/wiki/Doc/Config/IPSLCM6> (IGCMG, 2022), for a proper
520 installation and compilation of the environment (version 6.1.10).

521

522 **Data availability**

523

524 Pollen data are available on the African Pollen Database website:
525 <https://africanpollendatabase.ipsl.fr>. The other paleo-data are from the literature.

526

527 The IPSL-CM6A-LR model data and pre-processed model and proxies datasets used in this
528 study are available at: <https://doi.org/10.5281/zenodo.7003853>

529

530 **Author contribution**

531

532 AML and MK designed the study. MK performed the IPSL-CM6A-LR model past1000
533 simulations and JV the simulations analysis. MC and AML collected and analyzed the data.
534 AML prepared the manuscript with contributions from all co-authors.

535

536 **Competing interests**

537

538 The authors declare that they have no conflict of interest

539



540 **Acknowledgements**

541

542 This work contributes to the ACCEDE ANR Belmont Forum project (18 BELM 0001 05). This
543 work was undertaken in the framework of the French L-IPSL LABEX and the IPSL Climate
544 Graduate School EUR and benefited from the FNS “SYNERGIA EffeCts of lARge volcanic
545 eruptions on climate and societies: UnDerstanding impacts of past Events and related
546 subsidence cRises to evaluate potential risks in the future” (CALDERA) project under French
547 CNRS grant agreement number CRSII5_183571 – CALDERA. MK acknowledges support from
548 the HPC resources of TGCC under the allocations 2020-A0080107732 and 2021-A0100107732
549 (project genmip6) provided by GENCI (Grand Equipement National de Calcul Intensif) and
550 2020225424 provided by PRACE (Partnership for Advanced Computing in Europe). This study
551 benefited from the ESPRI computing and data centre (<https://mesocentre.ipsl.fr>) which is
552 supported by CNRS, Sorbonne Université, Ecole Polytechnique and CNES as well as through
553 national and international grants. Thanks are due to the African Pollen Database for data
554 access. AML, MC and JV were funded by CNRS, and MK by IRD. We acknowledge the World
555 Climate Research Programme's Working Group on Coupled Modelling.

556

557 **References**

- 558 Aguiar, L., Garneau, M., Lézine, A.-M., Maugis, P. Evolution de la nappe des sables quaternaires dans
559 la région des Niayes du Sénégal (1958-1994) : relation avec le climat et les impacts anthropiques.
560 *Sécheresse* 21, 1-8, 10.1684/sec.2010.0237, 2010.
- 561 Aumont, O., Éthé, C., Tagliabue, A., Bopp, L., and Gehlen : M. PISCES-v2. An ocean biogeochemical
562 model for carbon and ecosystem studies. *Geosci. Model Develop.*, 8(8), 2465-2513,
563 10.5194/gmd-8-2465-201, 2015.
- 564 Ballouche, A. : Dynamique des paysages végétaux sahélo-soudaniens et pratiques agro-pastorales à
565 l'Holocène : exemples au Burkina Faso. *Bull. Asso. Géogr. Français*, 75(2), 191-200, 1998.
- 566 Bertaux, J., Sifeddine, A., Schwartz, D., Vincens, A., and Elenga, H. : Enregistrement sédimentologique
567 de la phase sèche d'Afrique Equatoriale c. 3000 BP par la spectrométrie IR dans les lacs Sinnda
568 et Kitina (Sud Congo). In *Dynamique à long terme des écosystèmes forestiers intertropicaux*,
569 Paris, ORSTOM, pp. 213-215, 1998.
- 570 Boucher, O., Servonnat, J., Albright, A.L., Aumont, O., Balkanski, Y., Bastrikov, V., Bekki, S., Bonnet, R.,
571 Bony, S., Bopp, L. et al (2020) Presentation and evaluation of the IPSL-CM6A-LR climate model.
572 *J. Adv. Mode.l Earth Syst.*, 12(7), e2019MS002010, 10.1029/2019MS002010, 2020.
- 573 Brncic, T.M., Willis, K.J., Harris, D.J., and Washington, R. : Culture or climate? The relative influences
574 of past processes on the composition of the lowland Congo rainforest. *Philosoph. Trans. Royal*
575 *Soc. B., Biol. Sci.*, 362(1478), 229-242, 10.1098/rstb.2006.1982, 2007.
- 576 Brncic, T.M., Willis, K.J., Harris, D.J., Telfer, M.W., and Bailey, R. M. Fire and climate change impacts on
577 lowland forest composi-tion in northern Congo during the last 2580 years from palaeoeco-
578 logical analyses of a seasonally flooded swamp. *Holocene*, 19, 79–89,
579 10.1177/0959683608098954, 2009.
- 580 Carré, M., Azzoug, M., Zaharias, P., Camara, A., Cheddadi, R., Chevalier, M., Fiorillo, D., Gaye, A.T.,
581 Janicot, S., Khodri, M., Lazar, A., Lazareth, C.E., Mignot, J., Mitma Garcia, N., Patris, N., Perrot,
582 O., and Wade, M. : Modern drought conditions in western Sahel unprecedented in the past 1600
583 years. *Climate Dynamics*, 52(3), 1949-1964 10.1007/s00382-018-4311-3, 2019.
- 584 Catrain, M. Le Petit Age de Glace en Afrique équatoriale : apport de l'étude palynologique des
585 sédiments du lac de Petpenoun, Cameroun. Unpublished Ms Thesis. University of Paris Saclay,
586 2021.
- 587 Coquery-Vidrovitch, C. : *Écologie et histoire en Afrique noire. Histoire, économie et société*, 483-504,
588 1997.



- 589 Descroix, L., Diogue Niang, A., Panthou, G., Bosdian, A., Sane, Y., Dacosta, H., Malam Abdou, M.,
590 Vandervaere, J.P., and Quantin, G.: Evolution récente de la pluviométrie en Afrique de l'Ouest
591 à travers deux régions: la Sénégambie et le bassin du Niger moyen. *Climatologie* 12, 25-43, 2015.
- 592 d'Orgeval, T., Polcher, J., and de Rosnay, P.: Sensitivity of the West African hydrological cycle in
593 ORCHIDEE to infiltration processes. *Hydro. Earth Syst. Sci.*, 12(6), 1387-1401, 10.5194/hess-12-
594 1387-2008, 2008.
- 595 Demenocal, P., Ortiz, J., Guilderson, T., Adkins, J., Sarnthein, M., Baker, L., and Yarusinsky, M.: Abrupt
596 onset and termination of the African Humid Period: rapid climate responses to gradual
597 insolation forcing. *Quatern. Sci. Rev.*, 19(1-5), 347-361, 10.1016/S0277-3791(99)00081-5, 2000.
- 598 Elenga, H.: Végétation et climat du Congo depuis 24 000 ans B. P: analyse palynologique de séquences
599 sédimentaires du Pays Bateke et du littoral. PhD, Aix-Marseille III, 1992.
- 600 Elenga, H., Schwartz, D., Vincens, A., Bertaux, J., de Namur, C., Martin, L., Wirrmann, D. and Servant,
601 M.: Diagramme pollinique holocène du lac Kitina (Congo): mise en évidence de changements
602 paléobotaniques et paléoclimatiques dans le massif forestier du Mayombe. *C. R. Acad. Sci.*,
603 Série 2a, 323, 403-410, 1996.
- 604 Fofana, C.A.K., Sow, E., and Lézine, A.-M.: The Senegal River during the last millennium. *Rev.*
605 *Palaeobot. Palynol.* 275, 104175, 10.1016/j.revpalbo.2020.104175, 2020.
- 606 Folland, C.K., Palmer, T.N., and Parker, D.E.: Sahel rainfall and worldwide sea temperatures, 1901–85.
607 *Nature*, 320, 602–607, 10.1038/320602a0, 1986.
- 608 Gallego, D., Ordóñez, P., Ribera, P., Peña-Ortiz, C., and García-Herrera, R.: An instrumental index of
609 the West African Monsoon back to the nineteenth century. *Quarter. J. Royal Meteor. Soc.*,
610 141(693), 3166-3176, 10.1002/qj.2601, 2015.
- 611 Giannini, A., Saravanan, R., and Chang, P.: Oceanic forcing of Sahel rainfall on interannual to
612 interdecadal time scales. *Science*, 302, 1027–1030, 10.1126/science.1089357, 2003.
- 613 Holmes, J.A., Allen, M.J., Street-Perrott, F.A., Ivanovich, M., Perrott, R.A., and Waller, M.P.: Late
614 Holocene palaeolimnology of Bal Lake, northern Nigeria, a multidisciplinary study. *Palaeogeogr.*
615 *Palaeoclimatol.*, Palaeoecol., 148(1-3), 169-185, 10.1016/S0031-0182(98)00182-5, 1999.
- 616 Hourdin, F., Rio, C., Grandpeix, J.Y., Madeleine, J.B., Cheruy, F., Rochetin, N., Jam, A., Musat, I., Idelkadi,
617 A., Fairhead, L., Foujols, M.A., Mellul, L., Traore, A.K., Dufresne, J.L., Boucher, O., Lefebvre, M.P.,
618 Millour, E., Vignon, E., Jouhaud, J., Diallo, F.B., Lott, F., Gastineau, G., Caubel, A., Meurdesoif, Y.,
619 and Ghattas, J.: LMDZ6A: the atmospheric component of the IPSL climate model with improved
620 and better tuned physics. *J. Adv. Model. Earth Syst.* 12(7): e2019MS001892,
621 10.1029/2019MS001892, 2020.
- 622 Jungclaus, J. H., Bard, E., Baroni, M., Braconnot, P., Cao, J., Chini, L. P., Egorova, T., Evans, M., Gonzalez-
623 Rouco, J.F., Goose, H., Hurtt, G.C., Joos, F., Kaplan, J.O., Khordi, M., Goldewijk, K.K., Krivova, N.,
624 LeGrance, A.N., Lorenz, S.J., Luterbacher, J., Man, W., Maucock, A.C., Mainshausen, M., Moberg,
625 A., Muscheler, R., Nehbass-Ahles, C., Otto-Bliesner, B.I., Phipps, S.J., Pongratz, J., Rozanov, E.,
626 Schmidt, G.A., Schmidet, H., Schmutz, W., Schurer, A., Shapiro, A.I., Sigl, M., Smerdon, J.E.,
627 Solanki, S.K., Timmreck, C., Toohey, M., Usoskin, I.L.G.L., Wagner, S., Wu, C.J., Yeo, K.L., Zanchettin,
628 D., Zhang, Q., and Zorita, E.: The PMIP4 contribution to CMIP6–Part 3: The last millennium,
629 scientific objective, and experimental design for the PMIP4 past1000 simulations. *Geosci. Model*
630 *Dev.*, 10(11), 4005-4033. 10.5194/gmd-10-4005-017, 2017.
- 631 Kageyama, M., Albani, S., Braconnot, P., Harrison, S. P., Hopcroft, P. O., Ivanovic, R. F., Lambert, F.,
632 Marti, O., Peltier, W.R., Peterschmitt, J.Y., Roche, D.M., Tarasov, L., Zhang, X., Brady, E.C.,
633 Haywood, A.M., LeGrande, A.N., Lunt, D.J., Mahowald, N.M., Mikolajewicz, U., Nisancioglu, K.H.,
634 Otto-Bliesner, B.L., Renssen, H., Tomas, R.A., Zhang, Q., Abe-Ouchi, A., Bartlein, P.J., Cao, J., Li,
635 Q., Lohmann, G., Ohgaito, R., Shi, X., Volodin, E., Yoshida, K., Zhang, X., and Zheng, W.: The
636 PMIP4 contribution to CMIP6–Part 4: Scientific objectives and experimental design of the
637 PMIP4-CMIP6 Last Glacial Maximum experiments and PMIP4 sensitivity experiments. *Geosci.*
638 *Model Dev.*, 10(11), 4035-4055, 10.5194/gmd-10-4035-2017, 2017.



- 639 Kanamitsu, M., Ebisuzaki, W., Woollen, J., Yang, S.-K., Hnilo, J.J., Fiorino, M., and Potter, G.L. : NCEP-
640 DOE AMIP-II Reanalysis (R-2), *Bull. Amer. Meteor. Soc.*, 83, 1631-1643, 0.1175/BAMS-83-11-
641 1631, 2002
- 642 Kucharski, F., Molteni, F., King, M.P., Farneti, R., Kang, I.S., and Feudale, L. : On the need of
643 intermediate complexity general circulation models : A “SPEEDY” example. *Bull. Amer. Meteo.*
644 *Soc.*, 94(1), 25-30, 10.1175/BAMS-D-11-00238.1, 2013.
- 645 Lawrence, D. M., Hurtt, G. C., Arneth, A., Brovkin, V., Calvin, K. V., Jones, A. D., Jones, C. D., Lawrence,
646 P. J., de Noblet-Ducoudré, N., Pongratz, J., Seneviratne, S. I., and Shevliakova, E.: The Land Use
647 Model Intercomparison Project (LUMIP) contribution to CMIP6: rationale and experimental
648 design, *Geosci. Model Dev.*, 9, 2973–2998, <https://doi.org/10.5194/gmd-9-2973-2016>, 2016.
- 649 Lebamba J., Vincens A., Lézine A.-M., Marchant R., and Buchet G. : Forest-savannah dynamics on the
650 Adamawa plateau (Central Cameroon) during the “African humid period” termination : A new
651 high-resolution pollen record from Lake Tizong. *Rev. Palaeobot. Palynol.*, 235, 129-139,
652 10.1016/j.revpalbo.2016.10.001, 2016.
- 653 Lenton, T.M. : Early warnin of climate tipping points. *Nature Climate Change* 1, 201-209,
654 10.1038/nclimate1143, 2011.
- 655 Lézine A.M., Lemonnier, K., and Fofana, C.A.K.: Sahel environmental variability during the last
656 millennium: insight from a pollen, charcoal and algae record from the Niayes area, Senegal. *Rev.*
657 *Palaeobot. Palynol.* 271, 104103, 10.1016/j.revpalbo.2019.104103, 2019.
- 658 Lézine A.M.: Late Quaternary vegetation and climate of the Sahel. *Quatern. Res.*, 32, 317-334,
659 10.1016/0033-5894(89)90098-7, 1989.
- 660 Lézine, A.M., Holl A., Lebamba J., Vincens A., Assi-Khadjis C., Février L., and Sultan E. : Temporal
661 relationship between Holocene human occupation and vegetation change along the
662 northwestern margin of the Central African rainforest. *C. R. Géosci.*, 345, 327-335,
663 10.1016/j.crte.2013.03.001, 2013.
- 664 Lézine, A.M., Lemonnier, K., Waller, M.P., Bouimetarhan, I., Dupont, L. and APD contributors : Changes
665 in the West African Landscape at the end of the African Humid Period. *Palaeoecology of Africa*
666 35, 65-83, 10.1201/9781003162766-6, 2021
- 667 Lézine, A.M., Zheng, W., Braconnot, P., Krinner, G.: Late Holocene plant and climate evolution at Lake
668 Yoa, northern Chad: pollen data and climate simulations. *Clim. Past* 7, 1351-1362, 10.5194/cp-
669 7-1351-2011, 2011.
- 670 Maley, J., and Vernet, R. : Peuples et évolution climatique en Afrique nord-tropicale, de la fin du
671 Néolithique à l’aube de l’époque moderne. *Afriques. Débats, Méthodes et Terrains d’Histoire*,
672 04, 10.4000/afriques.1209, 2013.
- 673 Matthes, K., Funke, B., Andersson, M. E., Barnard, L., Beer, J., Charbonneau, P., Clilverd, M. A., Dudok
674 de Wit, T., Haberleiter, M., Hendry, A., Jackman, C. H., Kretzschmar, M., Kruschke, T., Kunze, M.,
675 Langematz, U., Marsh, D. R., Maycock, A. C., Misios, S., Rodger, C. J., Scaife, A. A., Seppälä, A.,
676 Shangguan, M., Sinnhuber, M., Tourpali, K., Usoskin, I., van de Kamp, M., Verronen, P. T., and
677 Versick, S.: Solar forcing for CMIP6 (v3.2), *Geosci. Model Dev.*, 10, 2247–2302,
678 <https://doi.org/10.5194/gmd-10-2247-2017>, 2017.
- 679 Meinshausen, M., Vogel, E., Nauels, A., Lorbacher, K., Meinshausen, N., Etheridge, D. M., Fraser, P. J.,
680 Montzka, S. A., Rayner, P. J., Trudinger, C. M., Krummel, P. B., Beyerle, U., Canadell, J. G., Daniel,
681 J. S., Enting, I. G., Law, R. M., Lunder, C. R., O’Doherty, S., Prinn, R. G., Reimann, S., Rubino, M.,
682 Velders, G. J. M., Vollmer, M. K., Wang, R. H. J., and Weiss, R.: Historical greenhouse gas
683 concentrations for climate modelling (CMIP6), *Geosci. Model Dev.*, 10, 2057–2116,
684 <https://doi.org/10.5194/gmd-10-2057-2017>, 2017.
- 685 Mohino, E., Janicot, S., and Bader, J. : Sahel rainfall and decadal to multi-decadal sea surface
686 temperature variability. *Clim. Dyn.*, 37(3), 419-440, 10.1007/s00382-010-0867-2, 2011.
- 687 Mulitza, S., Heslop, D., Pittauerova, D., Fischer, H. W., Meyer, I., Stuut, J. B., Zabel, M., Mollenhauer,
688 G., Collins, J.A., Kuhnert, H., and Schulz, M. : Increase in African dust flux at the onset of



- 689 commercial agriculture in the Sahel region. *Nature*, 466(7303), 226-228, 10.1038/nature09213,
690 2010.
- 691 Nash, D.J., De Cort, G., Chase, B.M., Verschuren, D., Nicholson, S.E., Shanahan, T.M., Asrat, A., Lézine,
692 A.M., and Grab, S.W. : African hydroclimatic variability during the last 2000 years. *Quatern. Sci.*
693 *Rev.*, 154, 1-22, 10.1016/j.quascirev.2016.10.012, 2016.
- 694 Ngomanda, A., Jolly, D., Bentaleb, I., Chepstow-Lusty, A., M'voubou Makaya, Maley, J., Fortune, M.,
695 Oslisly, R., Rabenkogo, N. : Lowland forest response to hydrological changes during the last 1500
696 years in Gabon, Western Equatorial Africa. *Quatern. Res.* 60, 411-425,
697 10.1016/j.yqres.2008.12.002, 2007.
- 698 Nguetsop, V. F., Bentaleb, I., Favier, C., Martin, C., Bietrix, S., Giresse, P., Servant-Vildary, M., and
699 Servant, M. : Past environmental and climatic changes during the last 7200 cal yr BP in Adamawa
700 plateau (Northern-Cameroun) based on fossil diatoms and sedimentary carbon isotopic records
701 from Lake Mbalang. *Clim. Past*, 7(4), 1371-1393, 10.5194/cp-7-1371-2011, 2011.
- 702 Nguetsop, V.F., Bentaleb, I., Favier, C., Bietrix, S., Martin, C., Servant-Vildary, S., and Servant, M. : A
703 late Holocene palaeoenvironmental record from Lake Tizong, northern Cameroon using diatom
704 and carbon stable isotope analyses. *Quatern. Sci. Rev.*, 72, 49-62,
705 10.1016/j.quascirev.2013.04.005, 2013.
- 706 Nguetsop, V.F., Servant-Vildary, S., Servant, M., and Roux, M. : Long and short-time scale climatic
707 variability in the last 5500 years in Africa according to modern and fossil diatoms from Lake Ossa
708 (Western Cameroon). *Global Planet. Change*, 72(4), 356-367, 10.1016/j.gloplacha.2010.01.011,
709 2010.
- 710 Nicholson, S. E. The West African Sahel : A review of recent studies on the rainfall regime and its
711 interannual variability. *Intern. Scholar. Res. Not.*, 453521, 10.1155/2013/453521, 2013.
- 712 Nicholson, S.E. : Climatic variations in the Sahel and other African regions during the past five centuries.
713 *J. Arid Env.*, 1(1), 3-24, 10.1016/S0140-1963(18)31750-6, 1978.
- 714 Nicholson, S.E. : The nature of rainfall fluctuations in subtropical West Africa. *Monthly Weather Rev.*,
715 108(4), 473-487, 10.1175/1520-0493(1980)108<0473:TNORFI>2.0.CO;2, 1980.
- 716 Nicholson, S. E. : The West African Sahel : A review of recent studies on the rainfall regime and its
717 interannual variability. *Intern. Scholar. Res. Notices*, 2013, 453521, 10.1155/2013/453521,
718 2013.
- 719 Nicholson, S.E., Klotter, D., and Dezfuli, A.K. : Spatial reconstruction of semi-quantitative precipitation
720 fields over Africa during the nineteenth century from documentary evidence and gauge data.
721 *Quat. Res.*, 78, 13-23, 10.1016/j.yqres.2012.03.012, 2012
- 722 Pham-Duc, B., Sylvestre, F., Papa, F., Frappart, F., Bouchez, C. and Crétaux, J.F.: the Lake Chad
723 hydrology under current climate change. *Nature scientific Reports* 10, 5498, /s41598-020-
724 62417-w, 2020.
- 725 Reynaud-Farrera, I., Maley, J., and Wirrmann, D. : Végétation et climat dans les forêts du Sud-Ouest
726 Cameroun depuis 4770 ans BP : analyse pollinique des sédiments du Lac Ossa. *CR Acad. Sci. Paris*,
727 322(série II a), 749-755, 1996.
- 728 Rodríguez-Fonseca, B., Mohino, E., Mechoso, C. R., Caminade, C., Biasutti, M., Gaetani, M., Garcia-
729 Serrano J., Vizy E. K., Cook K., Xue Y. K., Polo I., Losada T., Druyan L., Fontaine B., Bader J., Doblas-
730 Reyes F. J., Goddard L., Janicot Serge, Arribas A., Lau W., Colman A., Vellinga M., Rowell D. P.,
731 Kucharski F., and Voltaire, A. : Variability and predictability of West African droughts: a review
732 on the role of sea surface temperature anomalies. *J. Clim.*, 28(10), 4034-4060, 10.1175/JCLI-D-
733 14-00130.1., 2015.
- 734 Rousset, C., Vancoppenolle, M., Madec, G., Fichefet, T., Flavoni, S., Barthélemy, A., Benshila, R.,
735 Chanut, J., Lévy, C., Masson, S., and Vivier, F. : The louvain-la-neuve sea ice model LIM3.6: global
736 and regional capabilities. *Geosci. Model. Dev.* 8(10), 2991-3005, 10.5194/gmd-8-2991-2015,
737 2015.



- 738 Salzmann, U., and Hoelzmann, P. : The Dahomey Gap: an abrupt climatically induced rain forest
739 fragmentation in West Africa during the late Holocene. *Holocene*, 15(2), 190-199,
740 10.1191/0959683605hl799rp, 2005.
- 741 Schefuß, E., Schouten, S., and Schneider, R.R. : Climatic controls on central African hydrology during
742 the past 20,000 years. *Nature*, 437(7061), 1003-1006, 10.1038/nature03945, 2005.
- 743 Shanahan, T.M., Overpeck, J.T., Anchukaitis, K.J., Beck, J.W., Cole, J.E., Dettman, D.L., Peck, J.A., Scholz,
744 A., and King, J.W. : Atlantic forcing of persistent drought in West Africa. *Science*, 324(5925), 377-
745 380, 10.1126/science.1166352, 2009.
- 746 Street-Perrott, F.A., Holmes, J.A., Waller, M.P., Allen, M.J., Barber, N.G.H., Fothergill, P. A., Harkness,
747 D.D., Ivanovich, M., Kroon, D. and Perrott, R.A. (2000). Drought and dust deposition in the West
748 African Sahel: a 5500-year record from Kajamarum Oasis, northeastern Nigeria. *Holocene*, 10(3),
749 293-302, 10.1191/095968300678141274, 2000.
- 750 Tovar, C., Harris, D.J., Breman, E., Brncic, T., and Willis, K.J. : Tropical monodominant forest resilience
751 to climate change in Central Africa: A Gilbertiodendron dewevrei forest pollen record over the
752 past 2,700 years. *J. Veget. Sci.*, 30(3), 575-586, 10.1111/jvs.12746, 2019.
- 753 Toohey, M., and Sigl, M.: Volcanic stratospheric sulfur injections and aerosol optical depth from
754 500 BCE to 1900 CE, *Earth Syst. Sci. Data*, 9, 809–831, 10.5194/essd-9-809-2017, 2017.
- 755 Villamayor, J., Mohino, E., Khodri, M., Mignot, J., and Janicot, S. : Atlantic control of the late
756 nineteenth-century Sahel humid period. *Journal of Climate*, 31(20), 8225-8240, 10.1175/JCLI-D-
757 18-0148.1, 2018.
- 758 Villamayor, J., M. Khodri, S-W Fang, J. Jungclaus, C. Timmreck and D. Zanchettin, Sahel droughts
759 induced by large volcanic eruptions over the last millennium in PMIP4/past1000 simulations.
760 Submitted.
- 761 Vincens, A., Buchet, G., Elenga, H., Fournier, M., Martin, L., de Namur, C., Schwartz, D., Servant, M., and
762 Wirrmann, D. : Changement majeur de la végétation du lac Sinnda (vallée du Niari, Sud Congo)
763 consécutif à l'assèchement climatique holocène supérieur : apport de la palynologie. *C.R. Acad.*
764 *Sci. Paris*, 318, 1521-1526, 1994.
- 765 Vincens, A., Schwartz, D., Bertaux, J., Elenga, H., and de Namur, C. : Late Holocene climatic changes in
766 western equatorial Africa inferred from pollen from Lake Sinnda, southern Congo. *Quatern. Res.*
767 50(1), 34-45, 10.1006/qres.1998.1979, 1998.
- 768 Vincens, A., Schwartz, D., Elenga, H., Reynaud-Farrera, I., Alexandre, A., Bertaux, J., Mariotti, A., Martin,
769 L., Meunier, J.D., Nguetsop, F., Servant, M., Servant-Vildary, S., and Wirrmann, D. : Forest
770 response to climate changes in Atlantic Equatorial Africa during the last 4000 years BP and
771 inheritance on the modern landscapes. *Journal of Biogeography*, 26(4), 879-885,
772 10.1046/j.1365-2699.1999.00333.x, 1999.
- 773 Waller, M.P., Street-Perrott, F.A., and Wang, H. : Holocene vegetation history of the Sahel: pollen,
774 sedimentological and geochemical data from Jikariya Lake, north-eastern Nigeria. *J. Biogeogr.*,
775 34(9), 1575-1590, 10.1111/j.1365-2699.2007.01721.x, 2007.
- 776 Wang, H., Holmes, J.A., Street-Perrott, F.A., Waller, M.P., and Perrott, R. A. Holocene environmental
777 change in the West African Sahel : sedimentological and mineral-magnetic analyses of lake
778 sediments from Jikariya Lake, northeastern Nigeria. *J. Quatern. Sci.*, 23(5), 449-460,
779 10.1002/jqs.1154, 2008.
- 780
781